LA-6095-MS
Informal Report

UC- 79b
Reporting Date: September 1975
Issued: October 1975

The Consequences of Sodium Bond Loss from an LMFBR Carbide Fuel Element

by

Jerry F. Kerrisk

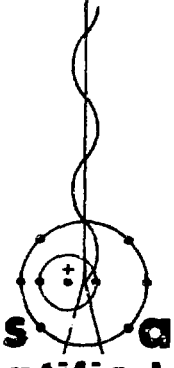

los alamos
scientific laboratory
of the University of California
LOS ALAMOS, NEW MEXICO 87545

UNITED STATES
ENERGY RESEARCH AND DEVELOPMENT ADMINISTRATION
CONTRACT W-7405-ENG. 36

In the interest of prompt distribution, this report was not edited by the Technical Information staff.

This work was supported by the U. S. Energy Research and Development Administration, Division of Reactor Research and Development.

Printed in the United States of America. Available from
National Technical Information Service
U S Department of Commerce
5285 Port Royal Road
Springfield, VA 22151
Price: Printed Copy $4.00 Microfiche $2.25

THE CONSEQUENCES OF SODIUM BOND LOSS FROM AN LMFBR CARBIDE FUEL ELEMENT

by

Jerry F. Kerrisk

ABSTRACT

The consequences of sodium bond loss from a uranium-plutonium carbide fuel element during normal steady state operation have been assessed. The elements considered are typical of those currently being irradiated in EBR-II, and include elements with and without shroud tubes. The analysis presented is very conservative in that the many simplifying assumptions required were made to predict worse consequences than would be found in a realistic analysis. Following sodium bond loss, fuel melting occurs, but the fuel rapidly resolidifies after slumping out to contact the clad. Even if molten fuel were lost through an existing clad failure, the maximum fuel temperatures attained are below those required to initiate a vapor explosion in the sodium coolant. The small amount of molten fuel that might escape through an existing clad failure would have little or no effect on adjacent elements.

1. INTRODUCTION

The uranium-plutonium carbide fuel system is a primary candidate for use as an advanced fuel in liquid metal fast breeder reactors. This fuel system offers significant advantages over uranium-plutonium oxide in reactor doubling time and breeding ratio, mainly due to the higher fissile atom density in the carbide fuel. There are two fuel element designs being actively studied using (U, Pu)C fuel.[1,2] A helium-bonded fuel element uses helium gas as the thermal bond between the fuel and the metallic (usually stainless steel) clad tubing. The initial fuel-clad diametral gap is small (usually less than 0.3 mm) so that fuel-clad mechanical interaction occurs during irradiation due to fuel swelling. Fuel centerline temperatures are in the range of 1400-2000°C initially, but drop during irradiation as the fuel-clad gap closes and better thermal contact is obtained. A sodium-bonded fuel element uses liquid sodium as the thermal bond between the fuel and clad. The initial fuel-clad diametral gap is normally in the range of 0.4 to 0.8 mm; this is large enough to allow fuel swelling without fuel-clad contact during the life of the element. The large gap is possible since the high thermal conductivity of liquid sodium results in very small temperature drops through the gap region. Fuel centerline temperatures are normally less than 1200°C.

A potential safety problem with sodium-bonded fuel elements is the behavior of the element following a loss of the sodium bond. The most probable cause of sodium bond loss is a clad failure below the sodium level in the element which allows the bond sodium to be lost to the coolant. At beginning of life, the pressure in the element plenum above the bond sodium will only be slightly higher than the coolant pressure. However, as

irradiation proceeds, fission gas will be released from the fuel so that end of life pressures in the element plenum can be much greater than those in the coolant. Thus throughout the fuel element life a driving force exists for sodium bond loss to the coolant. Following bond loss, the liquid sodium will be replaced by plenum gas. At the beginning of life this is pure helium; by the end of life the plenum gas is mostly fission gas (xenon and krypton), which has a much lower thermal conductivity than helium. The change from liquid sodium to plenum gas in the bond reduces the thermal conductance of the bond by about an order of magnitude; thus, high fuel temperatures and likely fuel melting will follow loss of sodium bond.

An added complication in considering the loss of the sodium bond is the presence of fuel fragment restraints or shroud tubes in elements.[2,3] Shroud tubes are perforated thin wall (less than 0.1 mm) tubes which fit around the fuel with a small diametral gap (approximately 0.05 mm). The shroud tubes are designed to prevent fuel fragments from cracked fuel pellets from rearranging inside the clad. Fuel fragment rearrangment and mechanical interaction with the clad during irradiation can lead to localized clad stresses. Some failures in sodium-bonded elements have been attributed to this phenomenon. Shroud tubes with a high melting point (tantalum) and with a low melting point (316 stainless steel) have been used.[3]

The object of this report is to assess the consequences of a loss of sodium bond from a carbide fueled element during normal steady state operation. The complexity of the initial fuel element state (for example, its burnup, fission gas release, fuel cracking pattern, gap size, and linear power) and the further complexity of the phenomena following bond loss preclude a realistic analysis of this accident. Thus the analysis here is meant as a conservative or limiting assessment of bond loss, and is not representative of what would actually happen. Many simplifying assumptions were made throughout the analysis; these assumptions were conservative in the sense that they tend to predict worse consequences than would result from a realistic analysis. Even with the series of conservative assumptions made, the consequences of sodium bond loss are far from catastrophic. Fuel melting can occur, but the fuel will resolidify on contact with the clad. Loss of sodium bond from a fuel element would have little or no effect on adjacent elements.

Section 2 of the report describes the nominal fuel element parameters and the steady state operating conditions of the fuel elements being analyzed. Section 3 discusses the consequences of a loss of bond through a clad failure during normal operation. This section is divided into discussions of a model used to calculate fuel and clad temperatures following bond loss and a presentation of the maximum fuel and clad temperatures calculated. Section 4 presents a calculation of the sodium coolant temperatures resulting from interaction with molten fuel that might escape from the element. Both instantaneous molten fuel-coolant interface temperatures and bulk coolant heating are considered. Section 5 contains a discussion of the overall analysis.

2. ELEMENT DESIGN AND NORMAL OPERATING CONDITIONS

The fuel elements considered here are based on the design of the "Series U5100 Singly Clad Carbide Experiments" which are being irradiated in EBR-II.[3] Each fuel element contains uranium-plutonium carbide fuel pellets enclosed in a metallic clad tube which is

7.14 mm (0.281 in) i.d. by
7.87 mm (0.310 in) o.d.

Some elements have shroud tubes. Each element is wire wrapped for coolant flow spacing in the subassembly. Table I lists a description of the fuel elements along with nominal operating conditions of each element. The linear power and fuel element temperatures were calculated using the PINTEMP code.[4] For the calculation, the subassembly (18 fuel elements and 1 dummy element) was assumed to be in core location 4B1 in EBR-II, with a total sodium flow of 4920 cm^3/s (78 gpm). The nominal fission rates for this location[5] were reduced by 9% to compensate for the latest estimates of actual EBR-II fission rates at 62.5 mW. The maximum goal burnup of these elements is 12 at.%.

TABLE I

U5100 SERIES ELEMENT PARAMETERS AND OPERATING CONDITIONS

Element Number	Fuel[a] Type	Fuel[b] Density % Theo.	Diametral[c] Gap, mm	Shroud[d]	Clad[e]	Peak Linear Power, kW/m	Peak Fuel Temp., °C	Peak Clad Temp., °C	Outlet[f] Na Coolant Temp., °C
U241	MC	94	0.46	None	304 SS	107	1035	565	466
U242	MC	93	0.44	None	304 SS	107	1040	576	477
U243	MC	93	0.80	None	304 SS	103	1030	559	463
U244	MC	93	0.44	None	304 SS	107	1035	565	466
U245	MC	93	0.81	None	304 SS	103	1033	569	473
U246	MC	93	0.43	None	316 SS	110	1058	581	480
U247	MC	93	0.81	None	316 SS	103	1027	558	463
U248	MC	93	0.81	None	316 SS	101	1022	565	471
U249	MC	93	0.43	None	INC-800	109	1057	581	479
U250	MC	93	0.81	None	INC-800	101	1055	628	536
U251	MC	93	0.81	None	304 SS	101	1056	629	537
U252	MC	93	0.64	V	304 SS	101	1028	566	471
U253	MC	93	0.66	Fe	304 SS	99	1046	624	533
U254	MC	93	0.66	304 SS	304 SS	99	1045	623	533
U256	MC+15%M_2C_3	96	0.61	V	304 SS	102	1017	557	462
U257	MC+15%M_2C_3	96	0.58	Ta	INC-800	101	1048	629	537
U258	MC+15%M_2C_3	96	0.58	304 SS	304 SS	101	1048	629	537
U259	MC+15%M_2C_3	96	0.58	304 SS	INC-800	103	1020	558	463

a. M = $(U_{.85}Pu_{.15})$.
b. Theoretical Density of MC = 13.45 g/cm^3; Theoretical Density of M_2C_3 = 12.72 g/cm^3.
c. The shroud thickness is not included in the diametral gap thickness.
d. Shroud tubes are 0.08 mm thick tubes with slots over 25% of the tube area.
e. All clad material is solution annealed.
f. The inlet Na temperature was assumed to be 371°C.

The fission gas content of the plenum gas and the total plenum pressure which would result during steady state irradiation were calculated for these elements for a number of assumed fission gas releases. For a plenum volume of 15 cm^3 there were 6 x 10^{-4} moles of helium in the plenum at fabrication (atmospheric pressure and 25°C). At 12 at.% burnup, 1.5 x 10^{-2} moles of fission gas (Kr + Xe) will be generated. Assuming a linear generation and release rate with burnup, the total plenum pressure and its composition can be calculated. Table II shows the results of this calculation. The helium content of the plenum gas will be used to estimate the thermal conductivity of the gas which replaces the sodium bond following bond loss. The total plenum pressure will be used to estimate the possible rate of molten fuel loss through a clad failure following bond loss.

The fuel-clad gap thickness will vary during steady state irradiation due to clad swelling and fuel swelling. Clad swelling was estimated for the fuel element conditions in EBR-II. Clad temperatures were taken from the steady state calculations using PINTEMP. Clad fluences were estimated using 7.2 x 10^{21} n/cm^2 (> 0.1 Mev) per at.% burnup (peak) at the core midplane, and 5.6 x 10^{21} n/cm^2 (> 0.1 Mev) per at.% burnup (peak) at the top of the core. Table III lists the range of clad swelling calculated for the elements in the subassembly as a function of burnup. The wide range results from the variation of clad material, fluence, and temperature throughout the subassembly. Fuel swelling was assumed to be a constant 3 vol% per at.% burnup. Using the clad swelling and fuel swelling estimates, the gap thickness can be calculated as a function of burnup. Initial gap thickness (at room temperature) ranged from 0.43 mm to 0.81 mm (see Table I). Table III also lists the maximum gap thickness calculated for elements with initial gaps of 0.43 mm and 0.81 mm. The maximum gap results from assuming the maximum clad swelling. Even using the maximum clad swelling rate, the fuel swells faster than the clad. Thus the gaps get smaller as irradiation proceeds.

TABLE II

U5100 ELEMENT PLENUM PRESSURE AND HELIUM CONTENT OF PLENUM GAS

% Fission Gas Release	Atom % Burnup	Plenum Pressure, atm	% Helium in Plenum Gas[a]
20	0	2.5	100
	3	6.4	45
	6	10.0	28
	9	13.5	21
	12	17.0	16
30	0	2.5	100
	3	8.0	35
	6	13.3	21
	9	18.5	15
	12	23.7	12
50	0	2.5	100
	3	11.5	24
	6	20.3	14
	9	29.0	10
	12	37.9	7

[a] The remainder of the plenum gas is fission gas (15% Kr and 85% Xe).

TABLE III

CLAD SWELLING AND GAP SIZE

Burnup at.%	Clad Volumetric Swelling, %	Maximum Gap mm	Maximum Gap mm
0	0	0.43	0.81
3	0 - 0.2	0.23	0.62
6	0 - 1.7	0.08	0.48
9	0.1 - 5.6	0.0	0.38
12	0.2 - 12.0	(a)	0.34

[a] Maximum burnup of small gap elements limited to 8 at.%.

3. LOSS OF BOND DURING NORMAL OPERATION

3.1 General Considerations

The cause of sodium bond loss considered is a clad defect which allows the bond sodium to be lost from the element into the coolant. The release would cause an increase in fission product activity in the coolant, and is thus detectable. The sequence of events involved is:

a. a clad defect occurring below the top of the fuel column,

b. the loss of the sodium bond through the defect into the coolant,

c. gas blanketing of the fuel by plenum gas which reduces the thermal conductance of the bond,

d. fuel (and shroud) melting if the linear power is high enough and the gap large enough,

e. slumping of the molten fuel (and shroud) against the clad which increases the thermal conductance of the bond, and

f. resolidification of the molten material.

Causes for concern during this sequence are possible clad melting from contact with the molten fuel, and the possible flow of molten fuel out the cladding defect into contact with the coolant sodium where a molten fuel coolant interaction (MFCI) can occur.

The likelihood of clad melting from contact with the molten fuel can be estimated from calculations of the clad surface temperature following contact with the molten fuel. Experimental evidence is also available from irradiation tests where molten fuel did contact cladding. The likelihood of a severe MFCI is mainly determined by the maximum fuel temperatures attained. If the molten fuel is hot enough to raise the sodium coolant temperature above its homogeneous nucleation temperature, then a vapor explosion is possible.

In the U5100 Series there are three groups of elements which could behave differently following a loss of bond:

a. the unshrouded elements, U241 through U251,

b. the elements shrouded with stainless steel, iron or vanadium, U252, U253, U254, U256, U258, and U259, and

c. the element shrouded with tantalum, U257.

This grouping is based on the presence or absence of a shroud tube and the melting point of the shroud tube. In the unshrouded elements there is nothing to restrict the slumping of the molten fuel out to the clad. In the elements shrouded with stainless steel (1425°C melting point), iron (1540°C melting point), and vanadium (1990°C melting point) the shroud material will melt before the fuel is completely molten (2440°C liquidus temperature). Thus the molten fuel and shroud can slump out to the clad. In the element shrouded with tantalum (2995°C melting point) the shroud will not be molten when the fuel starts to slump. Thus, the fuel will be forced to slump through the shroud tube slots to contact the clad.

The remainder of this section describes the models used to calculate the maximum fuel temperatures attained following a loss of bond, and the maximum clad temperatures attained following contact with molten fuel. The results for a variety of conditions are presented.

3.2 Heat Transfer Calculational Model

Heat transfer calculations were performed for three model elements:

a. an unshrouded element with 0.83 mm (33 mil) diametral gap between the fuel and clad i.d.,

b. an element with a 304 stainless steel shroud and a 0.53 mm (21 mil) diametral gap between the shroud o.d. and clad i.d., and

c. an element with a tantalum shroud and a 0.53 mm (21 mil) diametral gap between the shroud o.d. and clad i.d.

These are the largest initial gap sizes in this subassembly. Calculations were performed using initial gap sizes as a conservative assumption since these are the largest gaps during the life of the element. The element with the stainless steel shroud is also meant to cover the elements with iron and vanadium shrouds. Although the properties of vanadium are somewhat different than stainless steel, the outcome of the calculation is very insensitive to the shroud properties as long as the shroud has melted when the fuel has started to slump.

The calculations were one dimensional (radial) and assumed concentric fuel, shroud, and clad. The neglect of axial conduction and of the possibility of liquid sodium

remaining around the circumference of the bond is conservative in that it will predict higher fuel temperatures than if these other conduction paths were considered. The effect of pellet eccentricity was estimated by performing an approximate steady state calculation of the maximum fuel temperatures as a function of relative eccentricity (the ratio of pellet offset to the radial gap when concentric). A gas bond was assumed. Figure 1 shows the ratio of maximum fuel temperature with an eccentric pellet to the maximum for a concentric pellet, plotted as a function of relative eccentricity. It is evident that any eccentricity tends to reduce the maximum fuel temperature so that a concentric calculation is conservative.

The numerical heat transfer calculations which determined the maximum fuel temperatures and maximum clad temperatures used the CINDA code.[6] The node layout for the shrouded and unshrouded elements is shown in Fig. 2. The cold dimensions used were R_f = 3.15 mm, R_{si} = 3.213 mm, R_{so} = 3.302 mm, R_{ci} = 3.5687 mm, and R_{co} = 3.937 mm. The material properties are listed in Appendix A. The heat transfer coefficient to the flowing sodium coolant was assumed constant at 105 kW/m^2 ^{o}C.

The heat transfer calculations start at an initial steady state temperature distribution with the sodium bond intact. At zero time the gap sodium is completely replaced by plenum gas and a transient calculation follows the element temperatures. This is a conservative model since any liquid sodium remaining around the gap would provide a high conductance path to the clad and thus reduce the maximum fuel temperatures. The plenum gas was assumed to be 10% helium--90% fission gas. This amounts to an end of life (lowest thermal conductivity) composition with a 40% fission gas release. Both conduction and radiation were allowed across the gas regions. The fuel, shroud, and clad radii were corrected for thermal expansion in the steady state calculation and throughout the transient calculation. For the fuel thermal expansion calculation the fuel was assumed to be a solid pellet. The actual fuel with radial cracks will have a greater expansion. If fuel-shroud contact occurred while the fuel and shroud were still solid, the shroud was assumed to

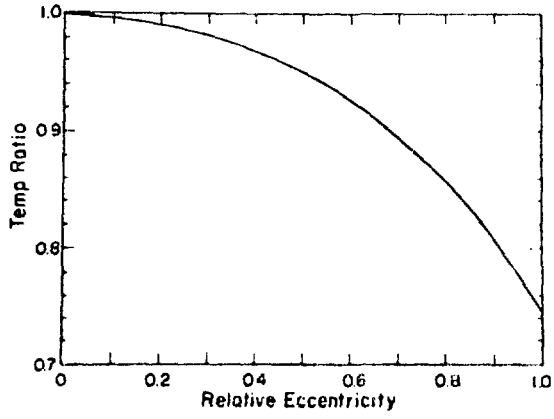

Fig. 1. Ratio of maximum fuel temperature with an eccentric pellet to the maximum for a concentric pellet as a function of relative eccentricity.

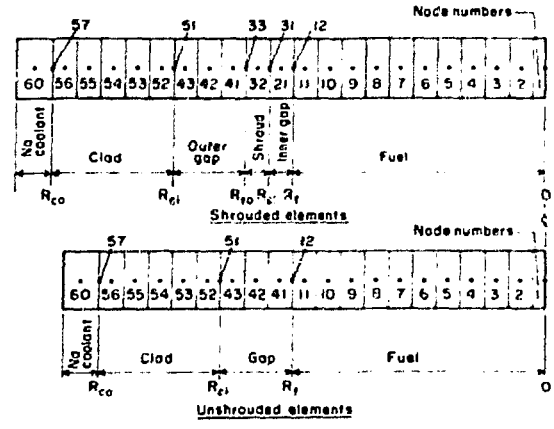

Fig. 2. Node geometry for heat transfer calculations.

break and continue to expand with the fuel. This occurred for the tantalum shroud since tantalum has a relatively low thermal expansion coefficient. The volume change on melting of the fuel is also accounted for by a modified thermal expansion coefficient in the melting range. This volume increase does not account for frothing of the fuel, but is solely a density change on melting. The heats of melting of the fuel and shroud are considered using adjusted heat capacities over the melting range.

Definition of what occurs once the fuel and shroud melt is difficult. For the purpose of temperature calculation two models were examined. In the first model the fuel and shroud were assumed to

maintain their structural integrity even though they had melted, i.e., no slumping was allowed. Calculations were performed with this model for the stainless steel shrouded element only. The thermal expansion and volume change on melting of the fuel and shroud were not sufficient to close the gas bond, so that the fuel and shroud attained a high steady state temperature. It is felt that this is an overly conservative model which bears no resemblance to what will actually occur, but the calculations were performed to provide some feeling for the influence of the model assumptions on the temperatures calculated. Results are shown in Section 3.3.

The second model used allows fuel slumping but is still considered conservative. The fuel was assumed to maintain its structural integrity until the fuel surface temperature was above its liquidus temperature, 2440°C. After this point, the fuel was allowed a specific time to slump out to the clad, depending on the condition of the shroud. If the shroud had melted, 0.1 s was allowed for the molten fuel and shroud to slump to the clad. This case covers the stainless steel, iron, and vanadium shrouds. If the shroud had not melted, 0.5 s was allowed for the molten fuel to slump through the shroud slots to the clad. This case covers the tantalum shroud. The unshrouded elements were also allowed 0.1 s to slump to the clad. These slumping times are considered conservative estimates of the time required for the molten fuel to move the short distances involved. They are greater than the estimates used in similar calculations of the melting of EBR-II metal fuel.[7] A justification for these time estimates is presented in Appendix B.

Once the fuel or shroud has contacted the cladding, a heat transfer coefficient must be defined between the contact surfaces. The following assumptions were used:

a. if two molten surfaces contact (e.g., fuel and shroud) or if a molten surface contacts a solid surface, a contact coefficient of 28.4 kW/m^2 °C (5000 Btu/h ft^2°F) was used,

b. if two solid surfaces contact, a contact coefficient of 5.7 kW/m^2 °C (1000 Btu/h ft^2 °F) was used,

c. when molten fuel contacted the clad through the still solid shroud tube, a contact coefficient of 5.7 kW/m^2 °C (1000 Btu/h ft^2 °F) was used to approximate the chance of reduced contact area (the shroud tubes have 25% slot area), and

d. once molten fuel or shroud material has contacted the clad, the contact was maintained.

The choice of 28.4 kW/m^2 °C for a solid-liquid contact coefficient is conservative for calculating peak fuel temperatures. This value is near the upper limit observed for solid-solid contact[9] and much less than values assumed to model molten fuel-clad contact with EBR-II metal fuel.[7] A low value for the conductance will restrict heat transfer and thus predict high fuel temperatures. For the calculation of peak clad temperatures following slumping of the fuel, the conservative predictions will result from large contact coefficients. To cover this limit, the peak clad temperatures following slumping in an unshrouded element were also calculated using a contact coefficient of 284 kW/m^2 °C (50,000 Btu/h ft^2 °F). The unshrouded element calculation was done since it predicts the highest peak clad temperature following slumping. This value for the contact coefficient approaches perfect thermal contact between the molten fuel and clad and provides upper limit estimates of the peak clad temperatures. The choice of 5.7 kW/m^2 °C for solid-solid contact is in the range of experimentally observed contact coefficients for solids.[8] None of the calculational results is sensitive to this choice.

3.3 Maximum Fuel and Cladding Temperatures

Heat transfer calculations were performed at two core locations, the core midplane where the element power is highest, and the top of the core where the sodium coolant temperature is highest. At the core midplane, the linear power was assumed to be 125 kW/m and the sodium temperature 450°C. At the top of the core, the linear power was assumed to be 110 kW/m and the sodium temperature 540°C. The linear powers are approximately 14% above the linear power of the highest powered element. This conservative assumption was made to account for uncertainties in reactor power and fission rates in the elements.

The major uncertainty in property data is the fuel thermal conductivity. To estimate the effect of this uncertainty, calculations were performed using fuel thermal conductivities of +20% and -20% in addition to the nominal values listed in Appendix A.

Table IV lists the maximum fuel (centerline) temperatures calculated for all the cases considered. For the cases where molten fuel slumping was allowed, the tantalum shrouded element shows the maximum fuel temperatures. This is due to the longer slumping time set for this case and the lower contact coefficient used once molten fuel-clad contact was established. The results for the unshrouded and stainless steel shrouded elements where slumping was allowed are quite similar. The results for the stainless steel shrouded element, where slumping was not allowed, are approximately 400°C higher than the similar cases where slumping was allowed. The small difference is mainly due to the fact that by the time slumping starts the fuel temperatures are beginning to peak out.

Figure 3 shows a plot of element temperatures as a function of time for the stainless steel shrouded element with the nominal fuel conductivity at the top of the core, with slumping allowed. Curve 1 is the fuel center, curve 2 is the fuel surface, curve 3 is the shroud mid-radius, and curve 4 is the clad inside surface. Shroud melting starts at about 1.1 s, fuel melting starts in the center at about 1.6 s, fuel-shroud contact occurs at 2.5 s, fuel and shroud slumping starts at 3.15 s, and contact with the clad is established at 3.25 s. The peak fuel temperature occurs in the center at about 3.4 s. Figure 4 shows a plot for the same conditions except that slumping was not allowed. Shroud melting, fuel melting, and fuel-shroud contact occur as in the previous case, but the molten fuel and shroud are assumed to maintain their integrity and not contact the clad.

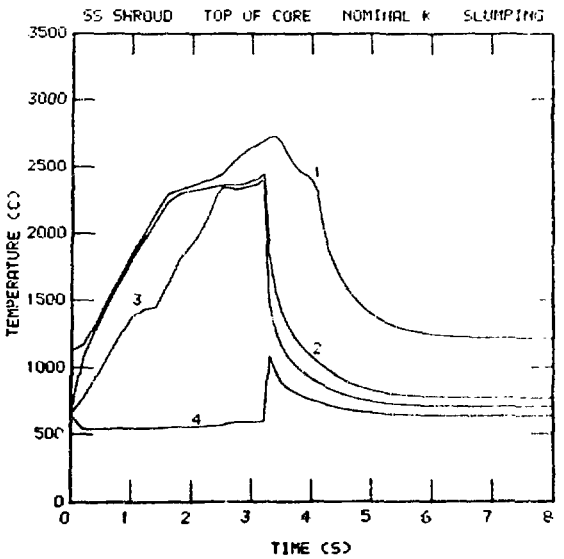

Fig. 3. Fuel element temperatures as a function of time following loss of bond with slumping allowed. (Curve 1 is fuel center, curve 2 is fuel surface, curve 3 is shroud mid-radius, and curve 4 is clad inside surface.)

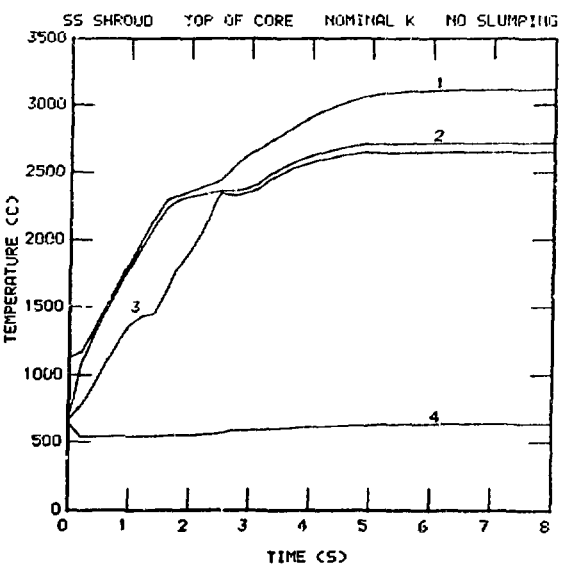

Fig. 4. Fuel element temperatures as a function of time following loss of bond with no slumping allowed. (Curve 1 is fuel center, curve 2 is fuel surface, curve 3 is shroud mid-radius, and curve 4 is clad inside surface.)

TABLE IV

MAXIMUM FUEL TEMPERATURES

Shroud	Fuel Slumping	Core Location [a]	Fuel Conductivity [b]	Maximum Fuel Temp., °C
Stainless Steel	Yes	M	N	2775
	Yes	M	+20%	2724
	Yes	M	-20%	2842
	Yes	T	N	2731
	Yes	T	+20%	2689
	Yes	T	-20%	2801
	No	M	N	3163
	No	M	+20%	3095
	No	M	-20%	3264
	No	T	N	3111
	No	T	+20%	3058
	No	T	-20%	3195
None	Yes	M	N	2702
	Yes	T	N	2677
	Yes	T	+20%	2648
	Yes	T	-20%	2720
Tantalum	Yes	M	N	3013
	Yes	T	N	2950
	Yes	T	+20%	2918
	Yes	T	-20%	2996

[a] M = Core Midplane, T = Top of Core.

[b] N = Nominal.

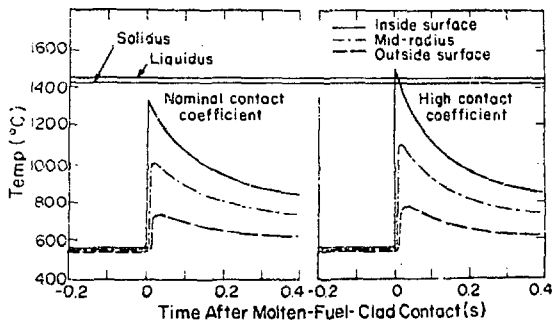

Fig. 5. Clad temperatures as a function of time after molten-fuel-clad contact for nominal and high contact coefficients.

The maximum clad temperatures calculated were for the unshrouded element, where molten fuel contacts the clad directly. Figure 5 shows a plot of clad temperatures as a function of time for an unshrouded element at the top of the core. The nominal contact coefficient is 28.4 kW/m^2 °C, while the high contact coefficient is 284 kW/m^2 °C. The inside surface temperature of the clad is above the melting range for a few milliseconds after contact, with the high contact coefficient. With the nominal contact coefficient, the entire clad is always below the melting range. It should be emphasized that the high contact coefficient is a conservative limiting case, i.e., it is essentially perfect contact between the molten fuel and clad.

4. SODIUM COOLANT TEMPERATURES FROM MOLTEN FUEL COOLANT INTERACTION

In this section, the molten fuel temperatures calculated in Section 3 are used to calculate possible sodium coolant temperatures resulting from an interaction of molten fuel and sodium. These calculations are aimed at estimating the likelihood of a homogeneous vapor explosion[9] or the possibility of bulk heating of the sodium above its boiling point. There are two temperature limits of interest for the sodium coolant. The first is the minimum sodium boiling temperature in the subassembly. The sodium pressure at the subassembly exit is approximately 1.5 atm (abs). To limit sodium coolant boiling at this pressure, the bulk sodium temperatures should be less than 925°C. The second limit, the homogeneous nucleation temperature of sodium, is 2300 K (2027°C). Even short time local sodium temperatures above this limit can cause rapid vaporization and possible shock waves in the sodium.

Section 4.1 discusses the calculation of the interface temperature between molten fuel and sodium. Section 4.2 discusses the calculation of bulk sodium coolant temperatures due to possible loss of molten fuel into the coolant channels.

4.1 Instantaneous Interface Temperatures

Using a model developed by Fauske,[10] the potential for achieving an instantaneous molten fuel-sodium interface temperature above the homogeneous nucleation temperature can be evaluated with the expression

$$\frac{T_i - T_s}{T_f - T_i} = \left[\frac{(k\rho c_p)_f}{(k\rho c_p)_s}\right]^{\frac{1}{2}} , \qquad (1)$$

where T is the temperature, k is the thermal conductivity, ρ is the density, c_p is the heat capacity, and subscripts s, f, and i refer to sodium, fuel, and the fuel-sodium interface, respectively. Interface temperatures were calculated for the maximum fuel temperatures shown in Table IV. This is a conservative assumption since the maximum fuel temperatures occur at the fuel centerline. Temperatures at the fuel surface adjacent to the clad failure are approximately 300°C below the fuel centerline temperatures. The sodium and fuel properties listed in Appendix A were used in the calculation. When an increased or decreased fuel thermal conductivity was used to calculate fuel temperatures, this same conductivity was used to evaluate the interface temperature. Figure 6 shows a plot of $\Delta T = 2027°C - T_i$ as a function of fuel thermal conductivity variation around its nominal values. The quantity ΔT can be considered as the safety margin between the calculated sodium interface temperatures and the homogeneous nucleation temperature of sodium. All the interface temperatures calculated are below the homogeneous nucleation temperature. The highest fuel temperatures calculated were at the core midplane (see Table IV). But the highest interface temperatures were calculated at the top of the core due

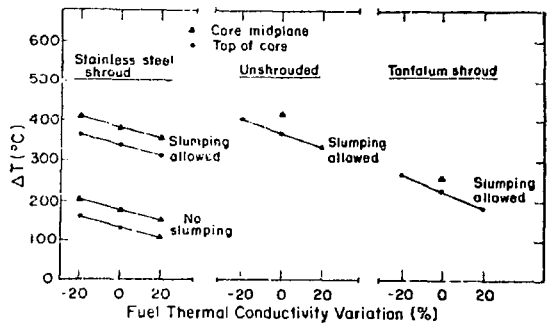

Fig. 6. Safety margin (ΔT) as a function of fuel thermal conductivity for a variety of conditions.

to the higher sodium coolant temperatures at this location. Thus, the smallest margin of safety (smallest ΔT) exists at the top of the core. As the fuel thermal conductivity increases, the maximum fuel temperatures calculated decrease (see Table IV). But this decrease in T_f is more than offset by an increase in the property ratio in Eq. (1). Thus, the interface temperatures increase (values of ΔT decrease) as the fuel thermal conductivity increases.

4.2 Bulk Heating of the Sodium

Even though the instantaneous interface temperature resulting from molten fuel-sodium contact is below the homogeneous nucleation temperature of sodium, it is possible that bulk heating of the sodium can raise its temperature above the boiling point. Bulk heating of the sodium will depend on the amount of molten fuel that is lost from the element and the rate of loss, as well as the molten fuel temperature. Estimates of the molten fuel loss in turn depend on the internal element pressure and the clad failure size.

The most uncertain quantity required for bulk heating estimates is the size of the clad failure. A number of failed elements with uranium-plutonium carbide fuel have been examined after irradiation. Most have come from encapsulated experiments in EBR-II,[11] but one element from the U5100 Series (U248) has failed and is being examined.[12] Five encapsulated elements (K-36B, K-45, K-46, B-3-3, and U194) have been examined which were known failures (fission gas was found in the capsule outside the element clad), but the failure point was never located.[11] One of the elements (K-45) was pressurized to 27 atm while heating the sodium bond above its melting point. These results indicate an extremely small failure but are not useful for a quantitative estimate of the failure size. A number of severely failed elements with large cracks in the clad and areas of melted clad have also been found during postirradiation examination of encapsulated fuel elements. A description of a mechanism by which slightly failed elements can progress to severe failures through interaction with the capsule has been presented.[11] The advanced fuel element failures observed to date have probably all started as slight failures. Continued irradiation after the initial failure produced the severe failures. Elements which are not encapsulated, such as the U5100 Series, are not subject to this same mechanism of failure progression from slight to severe.

Data obtained during the postirradiation examination of the U248 element are useful for estimating the size of the initial failure.[12] The element was pressurized internally and immersed in liquid. A small leak started at 24 atm pressure. During subsequent pressure testing, the failure leaked noticably at pressures as low as 17 atm. Data on the internal pressure loss of the element while it was closed off were used to estimate the failure size. For the calculation, the failure was assumed to be an orifice. The orifice flow formula used was[13]

$$Q = CA\sqrt{2\Delta P/\rho} \qquad (2)$$

where Q is the flow rate, A is the hole area, C is the orifice coefficient (0.6), ΔP is the pressure difference, and ρ is the density. The calculated size of the failure was 4×10^{-6} mm^2 at 24 atm and 1×10^{-6} mm^2 at 17 atm. The fact that the apparent failure size increases with increasing pressure is probably an indication that internal pressure tends to open the crack.

For the purpose of further calculation, two effective clad failure sizes have been chosen, a moderate failure size of 6×10^{-4} mm^2 (about two orders of magnitude greater than the estimate above) and a large failure size

of 6×10^{-2} mm^2 (about four orders of magnitude greater than the estimate above). These sizes are in the range used to characterize oxide element failures.[14]

To estimate the rate at which molten fuel might be lost through a moderate and large failure, Eq. (2) was again used with a molten fuel density of 10 g/cm^3 and a pressure differential of 70 atm. This essentially assumes complete fission gas release. Under these conditions the rate of molten fuel loss through a moderate failure would be 0.013 cm^3/s, and through a large failure would be 1.3 cm^3/s.

These estimates of molten fuel loss rates can be used in two ways, to estimate the total amount of molten fuel which might be lost from the element, and to estimate the bulk heating of the sodium coolant. As described in Section 3.2, when molten fuel contacts the cladding, the fuel is rapidly quenched. Solid fuel will plug any clad failure in a short time. To compute the time required to plug the failure, estimates of the linear failure size and the rate at which the solid-liquid interface in the fuel moves away from the fuel-clad interface are required. Assuming the clad failures are circular (which is conservative since it gives the largest linear dimension) the radius of the moderate failure is 1.4×10^{-2} mm and the radius of the large failure is 1.4×10^{-1} mm. The rate at which the solid-liquid interface in the fuel moves was obtained from the heat transfer model described in Section 3.2. For the contact of molten fuel (surface temperature 2520°C) with clad, the interface velocity is approximately 6.7 mm/s. An estimate of the time required to plug the moderate failure is

$$(1.4 \times 10^{-2} \text{ mm})/(6.7 \text{ mm/s}) = 2 \text{ ms},$$

and to plug the large failure is 20 ms. Using these time estimates, the moderate failure would release

$$(0.013 \text{ cm}^3/\text{s})(10 \text{ g/cm}^3)(0.002 \text{ s}) = 2.6 \times 10^{-4} \text{ g}$$

of fuel while the large failure would release 0.26 g of fuel.

The bulk heating of the sodium coolant will depend on the rate of loss of molten fuel from the element and the volume of sodium coolant with which it mixes. A conservative assumption would be that molten fuel is lost to a central subchannel of the subassembly and does not mix with other subchannels. The sodium flow in a central subchannel of the subassembly is 88 cm^3/s. The molten fuel loss rates are small and should not perturb the coolant flow rates significantly. If molten fuel of an average temperature T_f is mixed with sodium of temperature T_s, the final equilibrium temperature T_e of the mixture can be found from an energy balance,

$$m\,(\rho c_p)_f\,(T_f - T_e) = (1-m)(\rho c_p)_s\,(T_e - T_s),$$

where m is the volume fraction of fuel in the mixture. For the moderate failure

$$m \approx (0.013 \text{ cm}^3/\text{s})/(88 \text{ cm}^3/\text{s}) = 1.5 \times 10^{-4},$$

and for a large failure $m \approx 1.5 \times 10^{-2}$. This calculation of m ignores axial mixing and is, thus, conservative from that standpoint. For the calculations it was assumed that $T_f = 3000$°C, $T_s = 540$°C, $(\rho c_p)_f = 3.77$ J/cm^3 °C, and $(\rho c_p)_s = 0.837$ J/cm^3 °C.

The final equilibrium temperature of the fuel-sodium mixture is 542°C for the moderate failure and 700°C for the large failure. Both of these temperatures are below the boiling temperature of sodium at the subassembly outlet (925°C).

5. DISCUSSION

This report assesses the consequences of a loss of sodium bond from a uranium-plutonium carbide fueled element during normal steady state operation. The elements considered are typical of those currently being irradiated in EBR-II. The analysis includes elements with and without shroud tubes. Sodium bond loss into the coolant through a clad failure was the mechanism considered.

Maximum fuel temperatures were calculated and found to be in the range of 2700°C to 3000°C when fuel slumping is accounted for. If essentially perfect contact was allowed, inside clad surface temperatures above the melting range were calculated following contact with molten fuel. If less conservative estimates of the contact coefficient were used in the calculation, no clad melting was predicted. Sodium coolant temperatures calculated for instaneous contact with molten fuel and from bulk

heating were found to be below the homogeneous nucleation temperature for sodium. Bulk sodium coolant temperatures were also below the boiling temperature of sodium at the exit of the subassembly.

The peak cladding temperatures calculated here indicate the possibility of inside surface melting. There are two experiments which relate to this question. Gulf United Nuclear Fuels Corporation (GUNF) performed a set of GETR irradiations which examined the consequences of sodium bond defects and loss of bond.[15] Evidence of an interaction (probably due to inside clad surface melting) to about 0.05 mm out of 0.38 mm total clad thickness could be seen in some instances. No clad failures occurred in this group of elements. A LASL encapsulated element in EBR-II (K-49) was a severe failure and showed evidence of contact between possibly molten fuel and the capsule wall (316 SS).[11] There was no evidence of capsule melting or no interaction between the fuel and the capsule wall. The GUNF experiments tend to substantiate the calculations performed here, i.e., inside clad surface melting may occur from contact with molten fuel, but it is rapidly quenched as long as sodium coolant flow is maintained on the outside of the clad.

The molten fuel-coolant interaction (MFCI) calculations indicate that the sodium temperatures resulting from instantaneous contact with molten fuel will be 300°C to 400°C below the homogeneous nucleation temperature of sodium for unshrouded elements or those shrouded in stainless steel, iron, or vanadium. The tantalum shrouded element may have a smaller margin of safety. This result indicates that small amounts of fuel ejected from a clad failure will not cause homogeneous vaporization of the sodium coolant. Further calculations also indicate that bulk heating of the sodium coolant by molten fuel will not cause homogeneous vaporization or boiling of the sodium coolant.

Experiments performed by Atomics International have some bearing on these calculations.[16] TREAT tests overpowered sodium-bonded UC fuel in stainless steel clad which was surrounded by sodium and a heat sink. In one test, centerline fuel temperatures of 3150°C, with some indications of temperatures as high as 3800°C, were measured. The maximum pressure measured in the capsule was less than 13 atm. This transient overpower completely destroyed the element. Although these test results cannot be directly translated to the calculations presented here, they showed no significant MFCI under analogous conditions.

As concluding remarks, the generally conservative nature of the analysis presented here should be reiterated. In the calculation of the maximum fuel temperatures attained following the loss of bond, the effect of using initial gap sizes, concentric fuel and clad, complete loss of bond sodium, end of life (lowest thermal conductivity) plenum gas replacing the sodium, no axial conduction, power that is 14% above nominal, long slumping time for the fuel, and no frothing of the fuel on melting are all conservative. A partial retention of the sodium bond, significant axial conduction (due to a slow loss of bond), eccentric fuel in the clad, or shorter slumping times would all tend to reduce the maximum fuel temperatures calculated. An allowance for frothing (due to retained fission gas) of the central portion of the fuel at temperatures above its solidus temperature might even prevent melting of the outer region of the fuel. For these reasons the maximum fuel temperatures calculated should be considered as upper limits, and not necessarily representative of what would be attained following a loss of bond.

The estimates of the amount of fuel that could be lost through a clad failure and the loss rate are more speculative than the maximum fuel temperature calculations, but still represent a conservative calculation. Current evidence about initial clad failures indicates that they are much smaller than the hole sizes assumed in this analysis. The estimates presented should be considered as upper limits for initial failures, where the lower limit is no fuel lost.

ACKNOWLEDGMENTS

The author wishes to acknowledge the many discussions he had with John Barner concerning the ideas communicated in this report.

APPENDIX A

PROPERTY DATA

This appendix contains the property data used in the heat transfer calculations. Table A-1 lists the $(U_{.8}\ Pu_{.2})C$ fuel property data. Fuel thermal conductivity was obtained from an evaluation of experimental data from five sources.[17-21] Prior to evaluation, all the data were corrected to 100% theoretical density using the expression

$$k_p = k_o \frac{(1-p)}{(1+p)}$$

where k_o and k_p are the conductivities at zero pore volume fraction (100% theoretical density), and at pore volume fraction p, respectively. The volumetric heat capacity is the product of the heat capacity and density. Fuel density was calculated from the theoretical density of $(U_{.8}\ Pu_{.2})C$ at 25°C (13.43 g/cm³) and of $(U_{.8}\ Pu_{.2})_2C_3$ at 25°C (12.72 g/cm³). The effect of temperature on density was estimated from thermal expansion coefficient data,[22] and the density change on melting was estimated from data on inorganic salts with a similar structure.[23] The heat capacity of $(U_{.8}\ Pu_{.2})C$ fuel was calculated from the heat capacities of UC and PuC combined according to their mole fractions.[24] No emissivity data were found for carbide fuel, so a value of 0.5 was estimated. The liquidus and solidus temperatures of $(U_{.8}\ Pu_{.2})C$ have been measured.[25] The heat of fusion of $(U_{.8}\ Pu_{.2})C$ was estimated from an entropy of fusion of 5.5 eu.[26]

Table A-2 lists the stainless steel property data. These data can be used for 304 or 316 stainless steel. Standard reference sources were used for the thermal conductivity,[27] heat capacity,[28] thermal expansion coefficient,[29] density,[29] emissivity,[30] and melting temperatures[31] of stainless steel. The heat of fusion was estimated from the heats of fusion of the component elements.[32]

Table A-3 lists the tantalum property data. Standard reference sources were used for the thermal conductivity,[27] heat capacity,[28] thermal expansion coefficient,[33] density,[32] emissivity,[30] and melting point.[27]

Table A-4 lists the liquid sodium properties used. All data were obtained from a compilation of sodium property data.[34]

Table A-5 lists the properties of helium, argon, and fission gas used in the calculations. Fission gas was assumed to be 15% krpyton and 85% xenon. Thermal conductivity data for all four noble gases were taken from the same compilation.[35] Data for krypton and xenon were only available up to about 500°C. In the temperature range from 200°C to 500°C the ratio of the conductivity of krypton to that of argon is constant at 0.55, while the ratio of the conductivity of xenon to that of argon is constant at 0.35. Assuming these values hold over the entire temperature range of interest, and that the conductivity of a gas mixture can be obtained from the conductivities of its pure components by mole fraction averaging,

$$k_{fg} = (0.15)(0.55)k_A + (0.85)(0.35)k_A = 0.38k_A,$$

where k_{fg} and k_A are the thermal conductivities of fission gas and argon, respectively. Heat capacity data for all the gases were obtained from the same source.[36]

TABLE A-1

FUEL PROPERTY DATA

$(U._8 Pu._2)C$

Temperature ^{o}C	Volumetric Heat Capacity $J/cm^3\ ^{o}C$	Thermal Conductivity $W/cm\ ^{o}C$	Coefficient of Thermal Expansion $10^{-6}\ ^{o}C^{-1}$	Emissivity
204	2.97	0.146	8.9	0.5
427	3.11	0.167	10.0	0.5
649	3.19	0.185	10.8	0.5
871	3.27	0.198	11.2	0.5
1093	3.36	0.210	11.8	0.5
1316	3.44	0.218	12.2	0.5
1538	3.56	0.224	12.45	0.5
1760	3.69	0.228	12.7	0.5
1982	3.82	0.228	12.9	0.5
2204	3.95	0.228	13.1	0.5
2290 [a]	4.00	0.228	13.4 [c]	0.5
2291	19.87 [b]	0.228	13.4 [c]	0.5
2320	-	0.228	17.5 [c]	0.5
2365	18.45 [b]	0.228	25.8 [c]	0.5
2400	-	0.228	32.0 [c]	0.5
2440 [d]	16.57 [b]	0.228	39.2 [c]	0.5
2441	3.44	0.228	39.2 [c]	0.5
2704	3.59	0.228	36.8 [c]	0.5
2982	3.73	0.228	34.8 [c]	0.5
3427	3.85	0.228	33.7 [c]	0.5

[a] Solidus temperature.

[b] Simulates 243 J/g heat of fusion over 150°C temperature range.

[c] Simulates 20% volume increase on melting over 150°C temperature range.

d Liquidus temperature.

TABLE A-2

STAINLESS STEEL PROPERTIES

Temperature °C	Volumetric Heat Capacity J/cm³ °C	Thermal Conductivity W/cm °C	Coefficient of Thermal Expansion 10^{-6} °C^{-1}	Emissivity
204	3.03	0.167	16.9	0.2
427	3.12	0.203	17.8	0.2
649	3.34	0.241	18.7	0.2
871	3.52	0.276	19.5	0.2
1093	3.69	0.308	20.4	0.2
1316	3.74	0.341	21.2	0.2
1427 [a]	3.74	0.341	21.7	0.2
1428	74.90 [b]	0.341	21.7	0.2
1453	74.90 [b]	0.341	21.9	0.2
1454 [c]	3.77	0.341	21.9	0.2
1650	3.77	0.341	22.0	0.2

[a] Solidus temperature.

[b] Simulates 276 J/g heat of fusion over 27°C temperature range.

[c] Liquidus temperature.

TABLE A-3

TANTALUM PROPERTIES

Temperature °C	Volumetric Heat Capacity J/cm³ °C	Thermal Conductivity W/cm °C	Coefficient of Thermal Expansion 10^{-6} °C^{-1}	Emissivity
204	2.41	0.582	6.5	0.2
427	2.44	0.590	6.6	0.2
649	2.47	0.598	6.6	0.2
871	2.53	0.607	6.7	0.2
1093	2.60	0.615	6.8	0.2
1316	2.67	0.623	6.9	0.2
1538	2.73	0.632	7.1	0.2
1760	2.80	0.640	7.4	0.2
1982	2.90	0.649	7.7	0.2
2204	3.01	0.657	8.0	0.2
2426	3.18	0.665	8.3	0.2
2649	3.48	0.674	8.6	0.2
2871	4.13	0.682	8.9	0.2
2996 [a]	4.81	0.686	9.1	0.2

[a] Melting point.

TABLE A-4

LIQUID SODIUM PROPERTIES

Temperature °C	Volumetric Heat Capacity J/cm³ °C	Thermal Conductivity W/cm °C	Vapor Pressure atm
204	1.209	0.808	-
427	1.084	0.711	9.5×10^{-4}
649	1.000	0.611	6.8×10^{-2}
871	0.950	0.510	0.91
982	0.941	0.473	2.3
1093	0.933	0.435	5.0
1204	0.933	0.402	9.6
1316	0.933	-	16.9

TABLE A-5

HELIUM, ARGON, AND FISSION GAS PROPERTIES [a, c]

Temperature °C	Helium Thermal Conductivity W/cm °C	Fission Gas [b] Thermal Conductivity W/cm °C	Argon Thermal Conductivity W/cm °C
204	2.09×10^{-3}	9.6×10^{-5}	2.55×10^{-4}
427	2.78×10^{-3}	1.26×10^{-4}	3.35×10^{-4}
649	3.43×10^{-3}	1.55×10^{-4}	4.06×10^{-4}
871	4.02×10^{-3}	1.80×10^{-4}	4.69×10^{-4}
1093	4.60×10^{-3}	2.00×10^{-4}	5.23×10^{-4}
1316	5.19×10^{-3}	2.22×10^{-4}	5.82×10^{-4}
1538	5.73×10^{-3}	2.43×10^{-4}	6.40×10^{-4}
1760	6.32×10^{-3}	2.68×10^{-4}	7.03×10^{-4}
1982	6.82×10^{-3}	2.85×10^{-4}	7.49×10^{-4}
2204	7.32×10^{-3}	3.05×10^{-4}	8.08×10^{-4}
2527	8.08×10^{-3}	3.39×10^{-4}	8.87×10^{-4}
3027	9.16×10^{-3}	3.85×10^{-4}	10.13×10^{-4}

[a] Volumetric heat capacity of all noble gases taken as 8.45×10^{-4} J/cm³ °C based on a heat capacity of 20.8 J/mole °C and the gas density at 1 atm and 25°C.

[b] Fission gas composition is 15% Kr and 85% Xe.

[c] Gas mixture thermal conductivities calculated by weighing the individual conductivities by the mole fraction of the components.

APPENDIX B

FUEL SLUMPING TIME ESTIMATE

The time required for the molten fuel to slump out to the clad was based on a calculation of the potential energy difference between a volume of fuel before and after slumping, and the assumption that this potential energy difference was converted into kinetic energy, from which a fuel velocity could be estimated. Figure B-1 shows a diagram of a volume of fuel before and after slumping, where d_o and h_o are the initial diameter and height, and d_f and h_f are the final values. Assuming there is no volume change on slumping,

$$h_f = (d_o/d_f)^2 h_o .$$

The average potential energy change per gram of material in the volume on slumping is $\frac{1}{2}(h_o - h_f)$. The average kinetic energy per gram of materials is $V^2/2g$, where V is the velocity and g is the acceleration of gravity (980 cm/s^2). Equating the loss of potential energy with an increase in kinetic energy results in

$$V = [gh_o (1 - d_o^2/d_f^2)]^{\frac{1}{2}} .$$

This would be the final velocity achieved from the potential energy change. To calculate the slumping time, the average velocity V_a is needed. This was assumed to be half the final velocity,

$$V_a = \tfrac{1}{2}V = \tfrac{1}{2}[gh_o(1 - d_o^2/d_f^2)]^{\frac{1}{2}} .$$

The distance the fuel must move is $\frac{1}{2}(d_f - d_o)$, which is the radial gap. Therefore, the slumping time, t_s, is

$$t_s = \frac{\frac{1}{2}(d_f - d_o)}{V_a} = \frac{d_f - d_o}{[gh_o(1 - d_o^2/d_f^2)]^{\frac{1}{2}}} .$$

Calculations of the slumping time for various diametral gaps, and initial heights (h_o) of 1 and 10 mm are shown below:

	t_s (s)	
$(d_f - d_o)$ mm	h_o = 1 mm	h_o = 10 mm
0.05	0.004	0.001
0.25	0.01	0.003
0.50	0.014	0.004
0.75	0.017	0.006

The largest initial diametral gap (cold) is 0.83 mm. The largest diametral ga- the start of slumping is approximately 0.25 mm. This occurs in the unshrouded elements. The choice of t_s = 0.1 s for the unshrouded elements and the shrouded elements where the shroud has melted is about an order of magnitude greater than the estimate here for similar diametral gaps. The choice of t_s = 0.5 s for shrouded elements where the shroud has not melted is somewhat arbitrary, but it was felt that some penalty must be taken for slumping through the shroud holes.

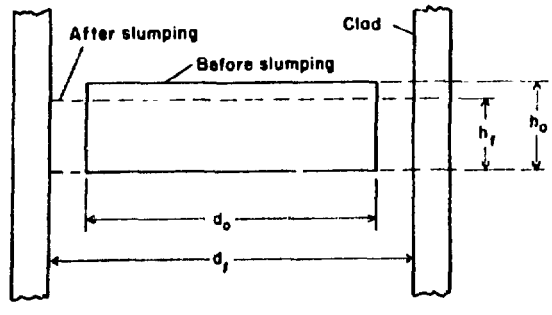

Fig. B-1. Fuel slumping diagram.

REFERENCES

1. T. W. Latimer, J. O. Barner, J. F. Kerrisk, and J. L. Green, "Steady-State Irradiation Behavior of Helium-Bonded Uranium-Plutonium Carbide," Trans. Am. Nucl. Soc. 19, 91 (1974).

2. J. O. Barner, T. W. Latimer, J. F. Kerrisk, D. Bost, and J. L. Green, "Steady-State Irradiation Behavior of Sodium-Bonded Uranium-Plutonium Carbide," Trans. Am. Nucl. Soc. 19, 91-92 (1974).

3. R. D. Baker, "Quarterly Report, Advanced Plutonium Fuels Program, January 1 through March 31, 1974," Los Alamos Scientific Laboratory report LA-5660-PR, pp. 16-18 (July 1974).

4. J. F. Kerrisk, "PINTEMP, A Computer Program for Fuel Element Design Calculations," Los Alamos Scientific Laboratory report, LA-5868-MS (February 1975).

5. "Guide for Irradiation Experiments in EBR-II," Argonne National Laboratory, EBR-II Project, Chicago, IL.

6. R. J. Connor, R. E. Kannady, Jr., and J. E. Almanza, "Adaptation of Chrysler Improved Numerical Differencing Analyzer to CDC 6000 Series Computers," Martin Marietta Corporation, report M-68-22 (November 1968).

7. C. E. Dickerman, F. L. Willis, R. R. Smith, P. B. Benault, R. Purviance, J. F. Boland, A. DeVolpi, R. A. Noland, J. Regis, A. B. Cohen, and C. M. Walter, "TREAT Sodium Loop Experiments on Performance of Unbonded, Unirradiated EBR-II Mark I Fuel Elements," Nucl. Eng. Design 12, pp. 381-390 (1970).

8. W. M. Rohsenow and J. P. Hartnett, Handbook of Heat Transfer (McGraw-Hill Book Co., New York, 1973), pp. 3-14 to 3-18.

9. L. C. Witte, "The Vapor Explosion," Journal of Metals, pp. 39-44, February 1970.

10. H. K. Fauske, "The Role of Nucleation in Vapor Explosions," Trans. Am. Nucl. Soc. 15, 813 (1972).

11. R. D. Baker, "Quarterly Report, Advanced Plutonium Fuels Program, April 1 through June 30, 1973, and Seventh Annual Report, FY 1973," Los Alamos Scientific Laboratory report LA-5390-PR, pp. 22-28 (September 1973).

12. J. O. Barner, Los Alamos Scientific Laboratory, private communication, 1974.

13. R. B. Bird, W. E. Stewart, and E. N. Lightfoot, Transport Phenomena (John Wiley and Sons, Inc., New York, 1960), pp. 224-226.

14. L. M. McWethy, "Fuel Failure Predictions and Consequences," General Electric report GEAP-13953, July 1973.

15. M. H. Montgomery, "High Power and Heat Flux Irradiation of Uranium-Plutonium Carbides," Gulf United Nuclear Fuels Corp. report GU-5294 (April 1973).

16. S. J. Stachura, M. Silberberg, and R. N. Cordy, "Uranium Carbide Transient Heating Studies - Phase II," Trans. Am. Nucl. Soc. 8, 305 (1965); S. J. Stachura and M. Silberberg, "The Application of Experimental Data from TREAT Meltdown Studies to Reactor Accident Analysis," Proceedings of the Conference on Safety, Fuels, and Core Design in Large Fast Power Reactors, Argonne National Laboratory report ANL-7120, pp. 514-523 (October 1965).

17. K. W. R. Johnson and J. A. Leary, "The Thermal Conductivity of Uranium Plutonium Carbides," Trans. Am. Nucl. Soc. 12, 591 (1969).

18. S. Bocker, R. Boucher, R. Lorenzelli, and C. Milet, "The U-Pu-C-M Carbides," in Plutonium 1970 and Other Actinides, W. N. Miner, Ed., (The Metallurgical Society of the American Institute of Mining, Metallurgical and Petroleum Engineers, New York, 1970) pp. 113-119.

19. J. C. Van Craynest, J. C. Weilbacher, and J. C. Salbreax, "Thermal Conductivity of Mixed Uranium and Plutonium Carbides, Nitrides, and Carbonitrides," Proceedings of the 8th Thermal Conductivity Conference, Purdue University, 1968, pp. 587-601.

20. R. Pascard, "Properties of Carbides and Carbonitrides," AIME Symposium on Plutonium Fuels Technology, Phoenix, Arizona, October 1967, pp. 345-368.

21. J. B. Moser and O. L. Kruger, "Thermal Diffusivity of Actinide Compounds," Proceedings of the 7th Thermal Conductivity Conference, Gaithersberg, Maryland, November 1967, pp. 461-467.

22. D. Stahl and A. Strasser, "Properties of Solid Solution Uranium-Plutonium Carbides," in Carbides in Nuclear Energy, L. E. Russell, et al., Eds., (MacMillan and Co., Ltd., London, 1964) pp. 373-391.

23. G. J. Janz, Molten Salts Handbook (Academic Press, New York, 1967), pp. 46-47.

24. E. K. Storms, The Refractory Carbides (Academic Press, New York, 1967), pp. 195 and 222.

25. "Quarterly Status Report on the Advanced Plutonium Fuels Program, April 1 through June 30, 1970, and Fourth Annual Report, FY 1970," Los Alamos Scientific Laboratory report LA-4494-MS, p. 26 (1970).

26. G. J. Janz, Molten Salts Handbook (Academic Press, New York, 1967), pp. 135-192.

27. Y. S. Touloukian, R. W. Powell, Y. C. Ho, and P. G. Klemens, Thermophysical Properties of Matter, Vol. 1, Thermal Conductivity, Metallic Elements and Alloys (Plenum Publishing Corporation, New York, 1970).

28. Y. S. Touloukian and E. H. Buyco, Thermophysical Properties of Matter, Vol. 4, Specific Heat, Metallic Elements and Alloys (Plenum Publishing Corporation, New York, 1970).

29. J. G. Conner and S. W. Porembka, "A Compendium of Properties and Characteristics for Selected LMFBR Cladding Materials," Battelle Memorial Institute report BMI-1900 (May 1968).

30. Y. S. Touloukian and D. P. DeWitt, Thermophysical Properties of Matter, Vol. 7, Thermal Radiative Properties, Metallic Elements and Alloys (Plenum Publishing Corporation, New York, 1970).

31. "Aerospace Structural Materials Handbook," Air Force Materials Laboratory report AFML-TR-68-115, Wright Patterson Air Force Base, Ohio (1971).

32 R. E. Bolz and G. L. Tuve, Eds., Handbook of Tables for Applied Engineering Science (The Chemical Rubber Company, Cleveland, 1970), pp. 96-97.

33. J. B. Conway and A. C. Losekamp, "Thermal-Expansion Characteristics of Several Refractory Metals to 2500°C," Trans. Met. Soc. AIME, 236, 702-709 (1966).

34. G. H. Golden and J. V. Tokar, "Thermophysical Properties of Sodium," Argonne National Laboratory report ANL-7323 (August 1967).

35. Y. S. Touloukian, P. E. Liley, and S. C. Saxena, Thermophysical Properties of Matter, Vol. 3, Thermal Conductivity, Non-Metallic Liquids, and Gases (Plenum Publishing Corporation, New York 1970).

36. Y. S. Touloukian and T. Makita, Thermophysical Properties of Matter, Vol. 6, Specific Heat, Non-Metallic Liquids, and Gases (Plenum Publishing Corporation, New York, 1970).